

This is the accepted manuscript made available via CHORUS. The article has been published as:

Coulomb enhancement of superconducting pair-pair correlations in a 3/4-filled model for κ -(BEDT-TTF)₂X

W. Wasanthi De Silva, N. Gomes, S. Mazumdar, and R. T. Clay

Phys. Rev. B **93**, 205111 — Published 9 May 2016

DOI: [10.1103/PhysRevB.93.205111](https://doi.org/10.1103/PhysRevB.93.205111)

Coulomb enhancement of superconducting pair-pair correlations in a $\frac{3}{4}$ -filled model for κ -(BEDT-TTF) $_2$ X

W. Wasanthi De Silva,¹ N. Gomes,² S. Mazumdar,² and R. T. Clay¹

¹*Department of Physics and Astronomy and HPC² Center for Computational Sciences,
Mississippi State University, Mississippi State MS 39762*

²*Department of Physics, University of Arizona, Tucson, AZ 85721*

(Dated: April 22, 2016)

We present the results of precise correlated-electron calculations on the monomer lattices of the organic charge-transfer solids κ -(BEDT-TTF) $_2$ X for 32 and 64 molecular sites. Our calculations are for band parameters corresponding to X = Cu[N(CN) $_2$]Cl and Cu $_2$ (CN) $_3$, which are semiconducting antiferromagnetic and quantum spin liquid, respectively, at ambient pressure. We have performed our calculations for variable electron densities ρ per BEDT-TTF molecule, with ρ ranging from 1 to 2. We find that d -wave superconducting pair-pair correlations are enhanced by electron-electron interactions only for a narrow carrier concentration about $\rho = 1.5$, which is precisely the carrier concentration where superconductivity in the charge-transfer solids occurs. Our results indicate that the enhancement in pair-pair correlations is not related to antiferromagnetic order, but to a proximate hidden spin-singlet state that manifests itself as a charge-ordered state in other charge-transfer solids. Long-range superconducting order does not appear to be present in the purely electronic model, suggesting that electron-phonon interactions also must play a role in a complete theory of superconductivity.

PACS numbers: 71.10.Fd, 71.10.Hf, 74.20.Mn, 74.70.Kn

I. INTRODUCTION

The family of layered organic superconductors κ -(BEDT-TTF) $_2$ X (hereafter κ -(ET)) has attracted strong interest because of its apparent similarity with the high T_c cuprates. As in the cuprates, superconductivity (SC) in κ -ET is proximate to semiconducting magnetic states, antiferromagnetic (AFM) or quantum spin liquid (QSL)¹. SC in the κ -(ET) $_2$ X as well as organic charge-transfer solids (CTS) in general is however reached by application of pressure rather than doping with charge carriers². Thus SC is a consequence of change of one or more parameters in the Hamiltonian that describes both the semiconducting and superconducting states, at fixed carrier concentration. The κ -ET lattice is strongly dimerized (see Fig. 1). Complete CT of one electron to the acceptor molecule X occurs from each dimer, which creates cations ET^{0.5+} with 0.5 holes (1.5 electrons) on each ET molecule. The dimer lattice is anisotropic triangular, and the magnetic behavior of the family can be understood within an *effective* $\frac{1}{2}$ -filled band Hubbard model. AFM in the strongly anisotropic X = Cu[N(CN) $_2$]Cl (hereafter κ -Cl), and QSL behavior in the nearly isotropic X = Cu $_2$ (CN) $_3$ (hereafter κ -CN) are both expected within the effective model¹.

In the context of the cuprates, there exists a large body of theoretical literature claiming that SC occurs within the Hubbard model³⁻⁵ for bandfilling slightly away from $\frac{1}{2}$, but no consensus has yet been reached on this matter. Similar mean-field and dynamic mean-field theories of κ -(ET) $_2$ X have proposed that SC also occurs within the exactly $\frac{1}{2}$ -filled band Hubbard model on an anisotropic triangular lattice⁶⁻¹⁴. A necessary condition for SC within any interacting electrons model however

is that interactions must enhance superconducting pair-pair correlations relative to the noninteracting model. Precise numerical calculations within the $\frac{1}{2}$ -filled band Hubbard model on triangular lattices have shown that pair-pair correlations decrease with Hubbard U for all anisotropy¹⁵⁻¹⁸, thus indicating the need for going beyond the effective 1/2-filled band model in our search for the mechanism of SC in κ -(ET) $_2$ X.

Recently an ubiquitous charge-ordered (CO) phase of unknown origin that competes with both AFM and SC has been discovered in the cuprates¹⁹⁻²⁴. The CO and SC orders have similar energy scales, and some investigators have suggested that “CO and SC appear as joint instabilities of the same normal state”²⁴. In the present work we report explicit calculations on multiple κ -ET lattices that are in apparent agreement with this hypothesis, in that we find the possible emergence of a superconducting state from a proximate hidden CO state. Uniquely for the case of carrier density precisely 0.5 or 1.5 per site, we have previously shown that there can occur a *spin-paired* CO state, a paired-electron crystal (PEC), in frustrated lattices^{25,26}. The PEC is a Wigner crystal of spin-bonded pairs, rather than of single electrons²⁷. In the κ materials, static PEC would require *unequal charge densities* on the monomer molecules that constitute each ET dimer, with *interdimer* spin-pairing between monomers with large charge densities^{25,26}. Such a static PEC has been observed in the κ compound X = Hg(SCN) $_2$ Cl $_2$ ²⁸. Other groups have proposed related theories of fluctuating intradimer charge disproportionation²⁹⁻³¹, in order to explain the peculiar dielectric responses of κ -CN³² and κ -Cl³³. Recent experiments have shown the absence of static CO in both materials³⁴, and ascribe the electrodynamic response of κ -CN to coupling of ET cations

to anions³⁵. These experiments, however, do not preclude local charge fluctuations driven *electronically* (with a timescale of 10^{-11} s or faster³⁴). Such charge fluctuations accompanies spin-singlet formation between neighboring charge-rich sites³⁶. Pair motion in this case involves exchange of electron population between pairs of charge-rich and charge-poor sites.

We have recently proposed that SC in the $(\text{ET})_2\text{X}$ evolves from a *paired-electron liquid* (PEL), which can be thought of as a destabilized PEC³⁶ (thus a static PEC is not a requirement for the PEL or SC.) We showed from precise numerical calculations that the pair-pair correlations are enhanced relative to the noninteracting limit uniquely for $\rho \simeq 0.5$. At all other ρ ($0 \leq \rho \leq 1$) pair-pair correlations are suppressed by the Hubbard U . Although the PEL does not have true long-range superconducting correlations, to the best of our knowledge this was the first demonstration of enhancement of pair-pair correlations within the Hubbard model.

The anisotropic triangular lattice lacks the strong dimerization of κ lattice, and the possibility of mapping to the effective $\rho = 1$ model³⁷ thus does not exist in this case. Whether or not Coulomb-induced enhancement of pair-pair correlations occurs in the *realistic* κ lattice, *also uniquely for the same carrier concentration* ρ , as well as the symmetry of the superconducting order parameter, if any, are of strong interest. We report here the results of such calculations of spin-spin and pair-pair correlations on the actual κ lattice, for realistic band parameters appropriate for $\kappa\text{-Cl}$ and $\kappa\text{-CN}$. As before³⁶, we perform these calculations for variable ρ . We demonstrate PEL formation on the κ lattices uniquely at or near $\frac{3}{4}$ filling with electrons, giving further credence to our proposal³⁶ that there occurs an effective electron-electron (e-e) attraction selectively at this ρ . To our knowledge, the present results report the first direct calculations of pair-pair correlations on large $\kappa\text{-ET}$ lattices.

The outline of the paper is as follows: in Section II we describe the theoretical model, the lattices and the computational methods we use; in Section III we present our computational results for the spin structure factor and pair-pair correlations in the ground state; and in Section IV we discuss our results in relationship to the current experimental data on $\kappa\text{-ET}$, as well as implications for theories of correlated-electron SC in general.

II. THEORETICAL MODEL, LATTICE, PARAMETERS, AND METHODS

As a minimal model for the electronic properties of the conducting layer of BEDT-TTF molecules in $\kappa\text{-ET}$, we consider the Hubbard Hamiltonian,

$$H = \sum_{\langle ij \rangle, \sigma} t_{ij} (c_{i, \sigma}^\dagger c_{j, \sigma} + H.c.) + U \sum_i n_{i, \uparrow} n_{i, \downarrow}. \quad (1)$$

In Eq. 1, $c_{i, \sigma}^\dagger$ ($c_{i, \sigma}$) creates (annihilates) an electron of spin σ on the highest MO of a *monomer* ET molecule i ,

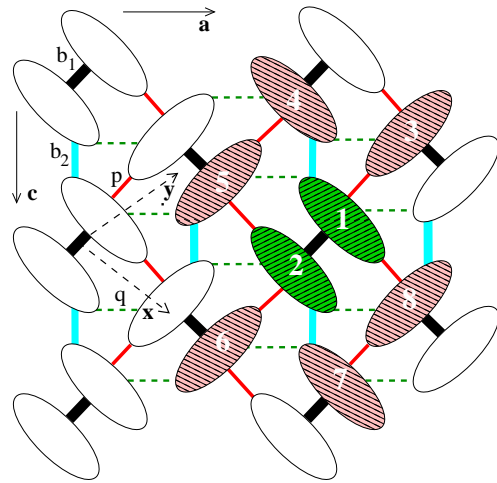


FIG. 1. (color online) Lattice structure of $\kappa\text{-(ET)}_2\text{X}$, showing individual monomer molecules. In order of decreasing magnitude, b_1 , b_2 , p , and q label the intermolecular hopping integrals. Superconducting pairs are constructed from the shaded molecules numbered 1 \cdots 8 as detailed in Section III B. The \mathbf{a} and \mathbf{c} crystal axes for $\kappa\text{-Cl}$ are indicated; for $\kappa\text{-CN}$ the corresponding axes are conventionally labeled \mathbf{b} and \mathbf{c} . The \mathbf{x} and \mathbf{y} axes for the effective dimer model are indicated by dashed arrows.

$n_{i, \sigma} = c_{i, \sigma}^\dagger c_{i, \sigma}$, and U is the onsite e-e interaction. The lattice structure³⁸ of the conducting layers in $\kappa\text{-ET}$ is shown in Fig. 1. In order to differentiate our approach from theories emphasizing the effective $\frac{1}{2}$ -filled band picture, in what follows instead of using the “bandfilling” we will present our computational results as a function of the average electron density per monomer molecule, ρ . As mentioned above, ρ in the $(\text{ET})_2\text{X}$ family is 1.5. While our calculations of the spin-spin correlations are for this density only, we have performed the calculations of superconducting pair-pair correlations for a wide range of ρ , $1 \leq \rho \leq 2$. The motivation behind studying the density dependence of pair-pair correlations is two-fold. First, this allows us to investigate whether or not SC is unique to $\rho \simeq 1.5$, which is a necessary condition if the SC is indeed evolving from a hidden PEC³⁶. Secondly, it also allows us to probe carrier density slightly away from the stoichiometric $\rho = 1.5$ in view of recent experiments³⁹ that have suggested that SC can occur in the $\kappa\text{-ET}$ system for weak doping away from $\rho = 1.5$.

Hopping integrals for $\kappa\text{-ET}$ have been previously calculated using the extended Hückel³⁸ and density-functional methods^{40–42}. Each molecule in the lattice has significant overlaps with six nearest neighbors (see Fig. 1) with hopping integrals t_{b1} , t_{b2} , t_p , and t_q in order of decreasing magnitude. In the effective dimer model the two molecules connected by t_{b1} are considered a single effective site, with the dimers forming an anisotropic triangular lattice. The effective hopping integrals along x and y are $t = (t_p + t_q)/2$ and the frustrating hopping integral $t' \equiv t_{-x+y} = t_{x-y} = t_{b2}/2$. The degree of frus-

tration in the effective dimer model is then given by the ratio $t'/t = t_{b2}/(t_p + t_q)$. Within the effective dimer model the frustration is weakest in κ -Cl and strongest in κ -CN. The ground states of both are very close to SC, as evidenced by the small pressures needed to reach the superconducting state. Note that the ambient pressure superconductor $X=\text{Cu}[\text{N}(\text{CN})_2]\text{Br}$ (κ -Br) is isostructural to κ -Cl: the difference between the calculated t_{ij} for κ -Cl and κ -Br is vanishingly small^{38,42} (mean-field calculations of magnetic correlations using the calculated t_{ij} on large κ -Cl and κ -Br lattices find AFM order in both⁴³, see below). For the strong e-e correlations we investigate here, small differences in bandstructure have little consequence. We therefore chose to consider κ -Cl and κ -CN, in order to cover the full range of frustration.

In our calculations we have used the following sets of t_{ij} , $(t_{b1}, t_{b2}, t_p, t_q)$, given in meV, from Reference 42: for κ -Cl (207, 67, -102, -43), and for κ -CN (199, 91, -85, -17). Both sets were determined⁴² from low-temperature crystal data, $T=5$ K in the case of κ -CN, and $T=15$ K in the case of κ -Cl. For these two sets of parameters, the ratio t'/t is 0.46 (0.89) for κ -Cl (κ -CN). While different computational techniques report somewhat different t'/t , all have found that in terms of the effective dimer model κ -CN is significantly more frustrated and closer to an isotropic triangular dimer lattice than is κ -Cl. It is however not known how the effect of the larger frustration within the dimer model affects the electronic properties of the full monomer lattice.

We considered two different periodic lattices with 32 and 64 molecular sites. The 32 site lattice is four dimers each along the **c** and **a** directions in Fig. 1. The lattice is chosen such that the effective dimer lattice (along the **x** and **y** axes of Fig. 1) is a 4×4 square lattice. This is possible if the vectors defining the edges of the 32 site cluster are along the **c** and **y** directions in Fig. 1. The 64 site cluster was constructed in a similar way and corresponds to an 8×4 lattice in terms of dimers. The full lattices are shown in the Supplemental Material⁴⁴. On both lattices, the t_{ij} parameters⁴² for κ -Cl and κ -CN gave different single-particle Fermi level degeneracies; the degeneracy for $\rho = 1.5$ is twofold in κ -Cl and fourfold in κ -CN, in agreement with the greater frustration in the latter.

Conventional quantum Monte Carlo methods cannot be used in the highly frustrated κ -ET lattice due to the fermion sign problem. The two methods we used are the Path Integral Renormalization Group (PIRG)⁴⁵ and Constrained Path Monte Carlo (CPMC)⁴⁶. Both PIRG and CPMC are ground state projector methods that project out the ground state from an arbitrary initial wavefunction. In PIRG the projection is done in a finite basis of Slater determinants, followed by an extrapolation in the energy variance⁴⁵. In CPMC the projection is done using random walkers constrained by a trial wavefunction⁴⁶. Here we have used the $U = 0$ wavefunction for the constraint. We have extensively benchmarked calculations of superconducting pair-pair between these two methods in previous work on the

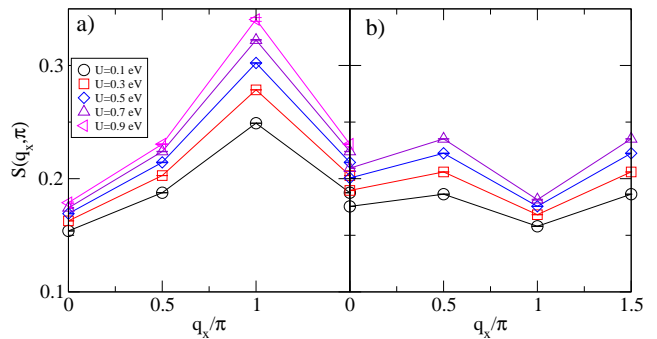


FIG. 2. (color online) Dimer spin structure factor $S(\mathbf{q})$ as a function of wavevector calculated using PIRG for $\rho=1.5$. Wavevectors are defined in terms of the effective dimer lattice with axes **x** and **y** as shown in Fig. 1. Panels are (a) 32 sites, κ -Cl, (b) 32 sites, κ -CN

anisotropic triangular Hubbard model both at $\frac{1}{2}$ -filling¹⁷ as well as the complete density range³⁶. While PIRG can be considered exact provided large enough basis sets are used and the projection is done with care, the constraining wavefunction in CPMC does introduce a systematic error. In our previous work, we found that CPMC results for pairing correlations agreed well with PIRG for small to intermediate U , provided use of CPMC was restricted to systems which in the noninteracting $U = 0$ limit have nondegenerate closed-shell Fermi level occupancies^{36,46}.

III. RESULTS

We performed PIRG calculations for the 32-site lattice over the full density range $1 < \rho < 2$ and for $\rho = 1.5$ for the 64-site lattice. For the other densities of the 64 site lattice with nondegenerate Fermi level occupancies we performed CPMC calculations. We used the full set of spatial symmetries within the symmetrized version of PIRG (QP-PIRG), which has been shown to significantly improve the results compared to earlier PIRG calculations⁴⁷. The symmetries we used for the 32 site lattice were translations, a π rotation, and a glide-plane symmetry. We also projected out the even spin parity state. The PIRG basis size was up to $L=512$ Slater determinants for 32 sites and $L=768$ for 64 sites.

A. Spin structure factor

AFM is best explained within the effective dimer model^{1,6-15}, where the charge densities on the molecules of the dimer are equal. Accordingly we define the total z -component of spin on dimer i as

$$S_i^z = \frac{1}{2}(n_{i_1,\uparrow} + n_{i_2,\uparrow} - n_{i_1,\downarrow} - n_{i_2,\downarrow}). \quad (2)$$

In Eq. 2, i_1 and i_2 refer to the two different molecules within the dimer i and $n_{j,\sigma} = c_{j,\sigma}^\dagger c_{j,\sigma}$. We calculate the

dimer spin structure factor defined as

$$S(\mathbf{q}) = \frac{1}{N_d} \sum_{j,k} e^{i\mathbf{q} \cdot (\mathbf{r}_j - \mathbf{r}_k)} \langle S_j^z S_k^z \rangle, \quad (3)$$

where N_d is the number of dimers and dimer position vectors \mathbf{r}_j are defined on a conventional square lattice, whose \mathbf{x} and \mathbf{y} axes are indicated on Fig. 1.

In Fig. 2 we show results for $S(\mathbf{q})$ for both κ -Cl (Fig. 2(a)) and κ -CN (Fig. 2(b)). $S(\mathbf{q})$ for κ -Cl has a peak at $\mathbf{q}=(\pi, \pi)$ consistent with Néel AFM correlations as expected in the $\rho = 1$ effective model for moderate frustration. As shown in Fig. 2(a), the (π, π) peak for κ -Cl grows with increasing U . In contrast, we found no clear magnetic ordering peak in $S(\mathbf{q})$ for κ -CN, consistent with the greater frustration within the effective dimer model in this case.

For the 64 site κ -Cl lattice $S(\pi, \pi)$ is smaller in magnitude than for 32 sites, and the peak appears somewhat broader in momentum space. At present we do not have access to large enough system sizes to perform a finite-size scaling for $S(\mathbf{q})$, but the decrease of $S(\pi, \pi)$ with increasing system size indicates that our κ -Cl results are consistent with a metallic state with AFM correlations rather than an AFM insulating state ($S(\pi, \pi)/N_d$ should scale to a non-zero value in the presence of long-range AFM order at $T = 0$ in the thermodynamic limit). We discuss this issue further in Section IV. For the 64 site κ -CN lattice, we find that the variation $S(\mathbf{q})$ with \mathbf{q} is less than for 32 sites; this behavior is consistent with lack of magnetic order in the Mott insulating state of κ -CN.

B. Pair-pair correlations

We calculate equal-time superconducting pair-pair correlations $P_{ij} = \langle \Delta_i^\dagger \Delta_j \rangle$, where Δ_i^\dagger creates a superconducting pair centered at dimer i . There are two requirements for a complete theory of correlated-electron superconductivity³⁶: (i) e-e correlations should enhance the value of P_{ij} compared to its uncorrelated value, and (ii) P_{ij} has long-range order at $T = 0$. Here we focus on (i).

As mentioned above, previous works have shown (i) suppression of pair-pair correlations within the effective $\rho = 1$ model^{15–18}, and (ii) the possibility of a fluctuating CO within models focusing on the monomer molecules^{25,26,29–31}. We therefore construct pair creation operators that allow unequal charge densities on the monomer molecules that constitute a dimer in Fig. 1. We consider the central dimer (molecules labeled 1 and 2) in Fig. 1. The pair operator Δ_1^\dagger for this dimer is the superposition of singlets between sites 1 and 2 and the surrounding sites $3 \cdots 8$. In order to restrict the number of terms in Δ_i^\dagger and simplify the calculation, we restrict the singlets to only the stronger interdimer bonds of the lattice, *i.e.* the t_{b_2} and t_p bonds (we ignore the weak t_q bonds). As an example, $d_{x^2-y^2}$ singlet pairs (labeled d_1

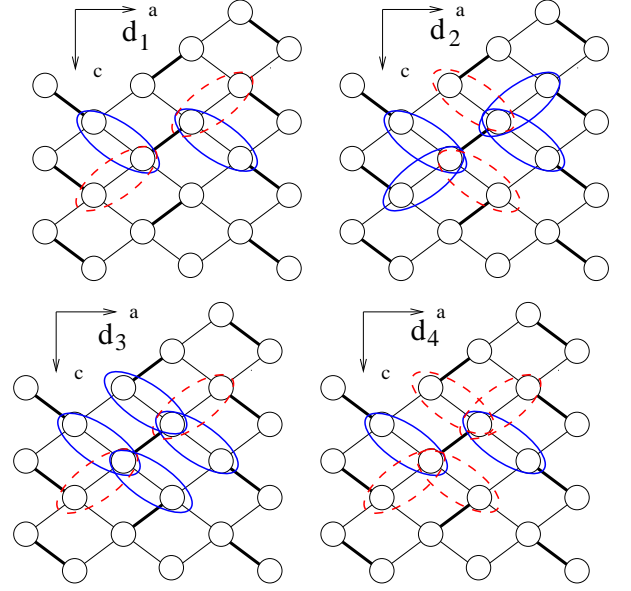


FIG. 3. (color online) Pairing symmetries considered in our calculations. Each ellipse surrounding two sites indicates the location of a singlet in the superposition for the pair operator Δ^\dagger . Blue, solid (red, dashed) singlets have opposite signs.

here, see below) similar to the conventional definition in the square effective lattice can be defined as follows for the dimer (1,2) in Fig. 1,

$$\begin{aligned} \Delta_{d_1}^\dagger = \frac{1}{2} \left[\frac{1}{\sqrt{2}} (c_{1,\uparrow}^\dagger c_{8,\downarrow}^\dagger - c_{1,\downarrow}^\dagger c_{8,\uparrow}^\dagger) \right. \\ - \frac{1}{\sqrt{2}} (c_{1,\uparrow}^\dagger c_{3,\downarrow}^\dagger - c_{1,\downarrow}^\dagger c_{3,\uparrow}^\dagger) \\ + \frac{1}{\sqrt{2}} (c_{2,\uparrow}^\dagger c_{5,\downarrow}^\dagger - c_{2,\downarrow}^\dagger c_{5,\uparrow}^\dagger) \\ \left. - \frac{1}{\sqrt{2}} (c_{2,\uparrow}^\dagger c_{6,\downarrow}^\dagger - c_{2,\downarrow}^\dagger c_{6,\uparrow}^\dagger) \right]. \quad (4) \end{aligned}$$

Given that the monomer lattice deviates strongly from the square lattice geometry several other pair symmetries are possible. Fig. 3 summarizes the pair symmetries we considered. These include four types of d -wave pairing (defined as symmetries with four nodes), with four as well as six neighbors. We do not show the results for s -wave pairing symmetries, as suppression of pair correlations were found with these, with four or six neighbors. The difference between the four d -wave pair symmetries we consider is in the locations of the nodes, which we discuss further in Section IV.

We calculate the average long-range value of the pair-pair correlations^{36,48} on each lattice, $\bar{P} = 1/N_P \sum_{|r_{ij}| > 2} P_{ij}$. Here N_P is the number of terms in the sum, and distances are defined in units of the nearest neighbor lattice distance of the effective dimer lattice. The restricted sum in the definition of \bar{P} is necessary to disentangle AFM and SC correlations. For the 32-site cluster for example, there are five P_{ij} separated by two

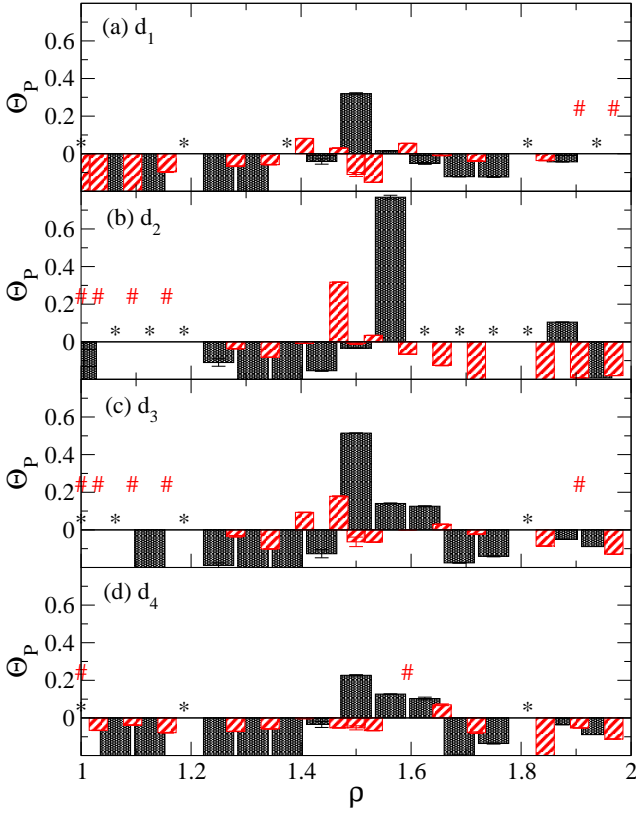


FIG. 4. (color online) The enhancement factor Θ_P for the long-range component of the pair-pair correlation ($\Theta_P > 0$ implies pair-pair correlations enhanced over their $U = 0$ values, see text), as a function of ρ , for the κ -Cl system for $U=0.5$ eV. Pair symmetries are (a) d_1 , (b) d_2 , (c) d_3 , and (d) d_4 as defined in Fig. 3. Shaded (striped) bars are for 32 (64) site lattices. The symbols ‘*’ and ‘#’ indicate densities not shown, for 32 and 64 sites, respectively; finite-size effects are particularly strong at these excluded ρ . Pair-pair correlations are suppressed by U at these excluded ρ , precluding pairing; see Supplemental Material⁴⁴.

or more lattice spacings in the equivalent 4×4 effective model.

In order to compare the extents of enhancements of pair-pair correlations by the Hubbard U at different densities we normalize \bar{P} by its value for $U = 0$, and show results for the enhancement factor $\Theta_P = [\bar{P}(U)/\bar{P}(U = 0)] - 1$. In Figs. 4 and 5 we have shown Θ_P as a function of ρ for $U = 0.5$ eV. The normalization of \bar{P} fails for certain densities, where due to finite-size effects $\bar{P}(U = 0)$ is identically zero or very small in magnitude. For this reason, in Fig. 4 and Fig. 5, we have excluded densities for which pair-pair correlations are very small in magnitude at nonzero U , or (b) pair-pair correlations are negative. The complete data including the points excluded in Figs. 4 and 5 for both the κ -Cl and κ -CN lattices, for 32 as well as 64 sites are shown in the Supplemental Material⁴⁴. As seen there suppression of pair-pair correlations with U occurs at any ρ that has been excluded. Most of the data we excluded are also for densities sig-

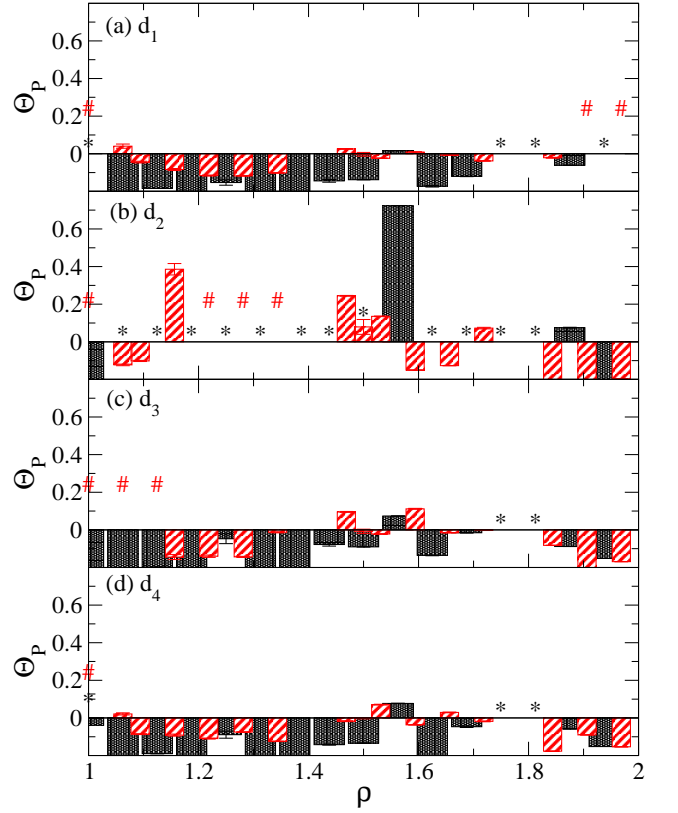


FIG. 5. (color online) Same as in Fig. 4, but for parameters for κ -CN. As in Fig. 4, behavior of all pair-pair correlations against U , including those for the excluded ρ are shown in the Supplemental Material⁴⁴. See text regarding the peak in panel (b) at $\rho \approx 1.16$; we believe the apparent enhancement here is a finite-size effect.

nificantly away from $\rho = 1.5$.

The results of Figs. 4 and 5 are remarkable, from multiple perspectives. First, in both cases suppression of \bar{P} is observed at all ρ except at or near $\rho = 1.5$, where there occur enhancements of \bar{P} . We are ignoring the enhancement seen in the 64-site data at $\rho = 1.156$ in Fig. 5(b). The full U -dependence for this point is in the Supplemental Material⁴⁴, Fig. S28. At this density, a discontinuous transition occurs at small U , suggesting a bandstructure effect. Furthermore at this ρ , \bar{P} for the d_2 symmetry is much smaller (but slightly above our cutoff) than for other symmetries. This and the fact that we do not see enhancement in any of our other results in the same density region suggests that it is a finite-size effect. Second, the strongest pairing enhancement occurs for the d_2 symmetry for both 32 and 64 sites. Finally, only for the d_2 pairing symmetry strong enhancement of \bar{P} at $\rho \simeq 1.5$ occurs for both the κ -Cl and κ -CN lattice parameters. This is a highly significant result, for as remarked above, the κ -Cl and κ -CN have different $U = 0$ single-particle level degeneracies at $\rho = 1.5$. It gives us confidence that the enhancement in pair correlations found here is not an artifact of the one-electron band structure.

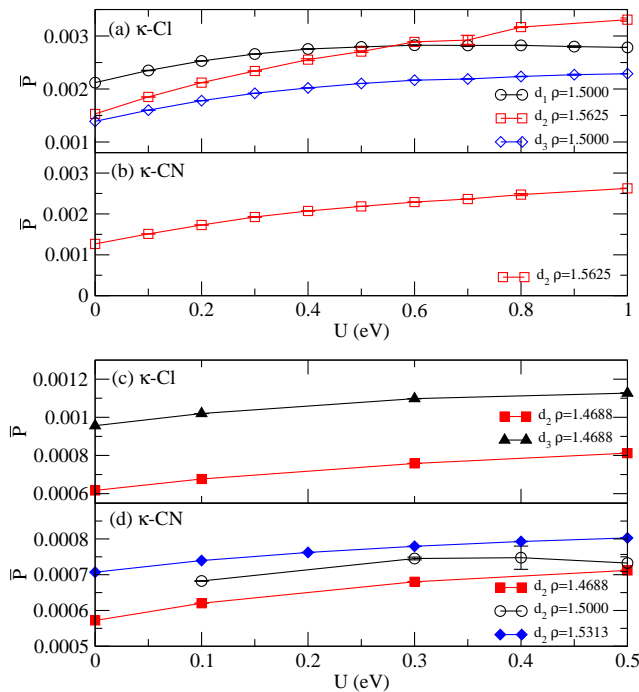


FIG. 6. (color online) U dependence of \bar{P} for densities showing significant enhancement of pair-pair correlations, for (a) κ -Cl, 32 sites, (b) κ -CN, 32 sites, (c) κ -Cl, 64 sites, and (d) κ -CN, 64 sites. all panels open (filled) symbols were calculated with PIRG (CPMC).

In Fig. 6 we show the complete U -dependence of \bar{P} at the densities where significant enhancements in pair-pair correlation occur, for both 32 and 64-site lattices, for both κ -Cl and κ -CN structures. Compared to the 32 site data, \bar{P} as well as Θ_P are smaller in magnitude for 64 sites, although we do expect that in the 64 site lattice \bar{P} will continue to increase at $\rho \approx 1.5$ for $U > 0.5$ eV. The Θ_P data however indicate the absence of true long-range superconducting order within our purely electronic model. If long-range superconducting order were present, \bar{P} would have reached a constant value with increasing system size, while $\bar{P}(U = 0)$ decreased, in which case Θ_P would be expected to increase with lattice size. The enhancement of pair-pair correlations uniquely at $\rho \simeq 1.5$ is nevertheless significant, because *this is precisely the carrier concentration in the superconducting κ -(ET) $_2$ X*. We elaborate on this aspect of our result further in the following section.

IV. DISCUSSIONS

We summarize our most significant results in this section, and discuss the implications of our work for κ -(ET) $_2$ X in particular, and for the family of two dimensional (2D) organic CTS in general.

A. AFM correlations versus long range AFM, and proximity to other broken symmetries

Mean-field calculations find long range AFM order within the monomer model we consider^{43,49}. While we do not have enough data to perform a finite-size scaling, the decrease of $S(\pi, \pi)$ with increasing system size suggests that the ground state of the present model does not have long-range AFM order, but is metallic with short-range AFM correlations (we cannot however rule out a very small AFM moment). We also did not find any evidence for a quantum phase transition to an AFM state in the 32-site lattice up to $U \approx 1$ eV. We ascribe the relative weakness of AFM correlations in our calculations to the well known tendency of mean field approaches to overestimate the stability of spin broken symmetry states, and underestimate the tendency to spin-singlet formation. Within the one-dimensional (1D) Peierls-Hubbard model for trans-polyacetylene, for example, mean-field calculations found the bond-alternated state replaced by a spin-density wave^{50,51} beyond a critical Hubbard $U \geq t_{ij}$, even as the correct result is that the spin-singlet bond-alternated state persists for all U ^{52–54}. While the calculated absence or weakness of AFM order appears counterintuitive, given the strong emphasis on AFM in theoretical works on these materials, it is in agreement with the experimental behavior of the κ -(ET) family as a whole. Experimentally, κ -Cl and deuterated κ -Br are the only compounds that exhibit AFM¹, and all other compounds are either ambient pressure superconductors (κ -Br² and κ -NCS²), QSL (κ -CN¹) or PEC (κ -Hg(SCN) $_2$ Cl²⁸). Several of the more complicated κ materials such as κ -(ET) $_4$ [M(CN) $_6$][N(C $_2$ H $_5$) $_4$]3H $_2$ O⁵⁵ and κ -(ET) $_4$ [M(CN) $_6$][N(C $_2$ H $_5$) $_4$]2H $_2$ O⁵⁶ (M = Co, Fe and Cr) are charge-ordered and spin-singlet, as in the PEC. Taken together, these results suggest that even as AFM spin-spin correlations in κ -ET are significant, these systems are at the threshold of transitions to proximate broken symmetries that include the PEC as well as SC. This observation is reminiscent of the occurrence of a CO phase competing with both AFM and SC in the cuprates^{19–24}.

We speculate that the origin of long range AFM in κ -Cl and deuterated κ -Br is due to either the nearest neighbor Coulomb interaction V , or the coupling between ET $_2^+$ cations and anions, both of which have been ignored in our calculations. Intradimer V promotes single electron occupancy of dimers, and therefore enhances AFM. Similarly, it is conceivable that cation-anion coupling enhances the extent of electron localization in the cation layer.

B. Enhancement of pair-pair correlations and carrier density

Our most significant result is the calculated enhancement of pair-pair correlations by Hubbard U within a narrow electron density range about $\rho = 1.5$. Enhanced

pair-pair correlations is a necessary though not sufficient condition for SC. We previously used this criterion to evaluate the possibility of SC within the $\rho = 1$ Hubbard model on triangular lattices^{15,17,18}. Suppression of pair-pair correlations by the Hubbard U was found for all the lattices we investigated. To the best of our knowledge, our results in Reference 36 for the first time showed an enhancement of pair-pair correlations within the single-band Hubbard model in large 2D clusters (up to 100 sites). It is then remarkable that we find here enhanced superconducting pair-pair correlations for two different κ lattices (κ -Cl and κ -CN), for two different lattice sizes in each case, *for precisely the same narrow carrier concentration range that would be anticipated from Reference 36*. This is particularly so considering the relevance of this carrier density to experimental (ET)₂X.

Within our theory, enhanced pair-pair correlations originate from the strong tendency to spin-singlet coupling at $\rho = 0.5$ and 1.5 , both because of the existence of a commensurate PEC at these densities^{25,26}, and because the stabilization due to the kinetic energy gain from pair motion is highest at these carrier concentrations. Thus within our theory, SC proximate to AFM (as occurs in the κ -(ET)₂X), as well as to CO (as occurs in other crystal structures or in the anionic superconductors⁵⁷⁻⁶⁰) are *manifestations of the same correlation effects and to be anticipated*.

C. PEL versus SC

Our work indicates that while repulsive e-e interactions can drive the transition to a PEL with short range pair-pair correlations at $\rho \simeq 1.5$, additional interactions missing in the purely electronic Hubbard model will be necessary to obtain long-range superconducting correlations. The most likely such interactions are that between the electrons and lattice vibrations involving intramolecular Holstein phonons⁶¹ and intermolecular Su-Schrieffer-Heeger (SSH) phonons⁶². We emphasize that there are many counterexamples to the notions that e-e and electron-phonon (e-p) interactions invariably negate each others effects and that e-p coupling can only generate SC of s -wave symmetry. One widely known counterexample is the co-operative enhancement of the e-p interaction driven Peierls bond-alternation in the 1D half-filled band by e-e interactions⁵²⁻⁵⁴. We have similarly found co-operative interactions between the effects of e-e and e-p interactions in the formation of the PEC in both one dimension⁶³ and two dimensions^{25,26}. In all these cases the retarded phonon interactions can be thought as “following” the instantaneous correlations driven by the e-e interactions. Thus the interpretation of our result that the PEL is unique to $\rho \simeq 1.5$ should be that in the presence of e-p interactions this is the carrier density in the κ lattice where correlated-electron SC is most likely. We also expect that the pairing symmetry will be determined primarily by the electronic system and

short-range e-e interactions (see also below). The situation is analogous to the $4k_F$ transition in the quasi-1D CTS, where nonzero e-p interactions are responsible for the actual lattice instability, but the periodicity of the distortion is determined by the e-e interactions⁶³.

D. Symmetry of superconducting order parameter

Experiments using a wide range of probes suggest that the SC pairing throughout the κ -(ET)₂X family is singlet with nodes in the order parameter. Experimental techniques that have been employed include site-selective ¹³C NMR^{64,65}, specific heat measurements⁶⁶, penetration depth measurements⁶⁷⁻⁶⁹, as well as STM tunneling experiments⁷⁰⁻⁷². While experiments are generally in agreement that the SC is singlet and has a nodal order parameter, there is less agreement on the specific form of the order parameter and the location of nodes in the conducting plane. Candidate symmetries $d_{x^2-y^2}$ and d_{xy} differ in the locations of their nodes; in the experimental literature $d_{x^2-y^2}$ symmetry is usually assumed to have nodes at 45° to the crystal axes, while d_{xy} has nodes along the crystal axes. It is important to note that in theoretical work based on the effective half-filled model, these two symmetries are interchanged, as the effective x and y axes are *rotated* with respect to the crystal axes (see Fig. 1). Magneto-optical⁷³ and specific heat measurements in a magnetic field find the nodes to coincide with the crystal axes⁷⁴. Thermal conductivity⁷⁵ and STM measurements^{70,71} however find the nodes between the crystal axes, although STM measurements on a partially deuterated κ -Br suggest a mixture of two order parameters⁷². Experiments sensitive to the position of the nodes have not been performed on κ -CN.

In our calculations (see Fig. 3), the d_1 symmetry has nodes along the crystal axes, while the d_2 symmetry instead has nodes at an angle between the crystal axes. The d_3 and d_4 have one node along a crystal axis and one off-axis. In our results we found the strongest enhancement for the symmetry d_2 , which is also the only symmetry with enhanced pairing for both κ -Cl and κ -CN. However, Fig. 4 shows that several pairing symmetries are enhanced for κ -Cl, suggesting the possibility that the optimum pairing symmetry may vary for different X in the κ -ET series, and that inclusion of e-p interactions will be needed to distinguish which of the symmetries d_1 - d_4 is most stable.

V. CONCLUSIONS

To summarize, from numerical calculations on the Hubbard model on the monomer lattice of κ -(ET)₂X solids we have found a PEL state with enhanced superconducting pair-pair correlations exactly for the cationic charge where SC is found experimentally in the (ET)₂X. We have also demonstrated that the pair-pair correla-

tions are suppressed by the Hubbard interaction at all other carrier densities. The superconducting order we find is short-range, and considerable work involving both e-e and e-p interactions will be necessary before a complete theory of SC in the CTS is reached. To the best of our knowledge, however, robust Coulomb enhancement of pair correlations has not been found before. Taken together with our previous work³⁶, this gives us confidence that the physical ideas behind this work, viz., (i) enhancement of superconducting pair correlations requires a proximate spin-singlet state in the phase diagram, and (ii) such a spin-singlet is strongly stabilized in two dimensions for $\rho = 0.5$ or 1.5 , are fundamentally correct.

VI. ACKNOWLEDGMENTS

S. M. and R. T. C. acknowledge very useful discussions with M. Dressel and S. Tomic, and for sending

them preprints of references 34 and 35. They are also grateful to N. Drichko for sending them the preprint of reference 28. This work was supported by the US Department of Energy grant DE-FG02-06ER46315. N. G. was supported by NSF grant CHE-1151475. Part of the calculations were performed using resources of the National Energy Research Scientific Computing Center (NERSC), which is supported by the Office of Science of the U.S. Department of Energy under Contract No. DE-AC02-05CH11231.

-
- ¹ K. Kanoda and R. Kato, *Annu. Rev. Condens. Matter Phys.* **2**, 167 (2011).
 - ² T. Ishiguro, K. Yamaji, and G. Saito, *Organic Superconductors* (Springer-Verlag, New York, 1998).
 - ³ P. W. Anderson, *Science* **235**, 1196 (1987).
 - ⁴ D. J. Scalapino, *Phys. Rep.* **250**, 329 (1995).
 - ⁵ P. W. Anderson, P. A. Lee, M. Randeria, T. M. Rice, N. Trivedi, and F. C. Zhang, *J. Phys. Condens. Matter* **16**, R755 (2004).
 - ⁶ M. Vojta and E. Dagotto, *Phys. Rev. B* **59**, R713 (1999).
 - ⁷ J. Schmalian, *Phys. Rev. Lett.* **81**, 4232 (1998).
 - ⁸ H. Kino and H. Kontani, *J. Phys. Soc. Jpn.* **67**, 3691 (1998).
 - ⁹ H. Kondo and T. Moriya, *J. Phys. Soc. Jpn.* **67**, 3695 (1998).
 - ¹⁰ B. J. Powell and R. H. McKenzie, *Phys. Rev. Lett.* **94**, 047004 (2005).
 - ¹¹ J. Y. Gan, Y. Chen, Z. B. Su, and F. C. Zhang, *Phys. Rev. Lett.* **94**, 067005 (2005).
 - ¹² P. Sahebsara and D. Sénéchal, *Phys. Rev. Lett.* **97**, 257004 (2006).
 - ¹³ T. Watanabe, H. Yokoyama, Y. Tanaka, and J. Inoue, *J. Phys. Soc. Jpn.* **75**, 074707 (2006).
 - ¹⁴ C. D. Hebert, P. Semon, and A. M. S. Tremblay, *Phys. Rev. B* **92**, 195112 (2015).
 - ¹⁵ R. T. Clay, H. Li, and S. Mazumdar, *Phys. Rev. Lett.* **101**, 166403 (2008).
 - ¹⁶ L. F. Tocchio, A. Parola, C. Gros, and F. Becca, *Phys. Rev. B* **80**, 064419 (2009).
 - ¹⁷ S. Dayal, R. T. Clay, and S. Mazumdar, *Phys. Rev. B* **85**, 165141 (2012).
 - ¹⁸ N. Gomes, R. T. Clay, and S. Mazumdar, *J. Phys. Condens. Matter* **25**, 385603 (2013).
 - ¹⁹ J. Chang *et al.*, *Nature Physics* **8**, 871 (2012).
 - ²⁰ S. Blanco-Canosa *et al.*, *Phys. Rev. B* **90**, 054513 (2014).
 - ²¹ M. Hücker *et al.*, *Phys. Rev. B* **90**, 054514 (2014).
 - ²² R. Comin *et al.*, *Science* **343**, 390 (2014).
 - ²³ E. H. D. S. Neto *et al.*, *Science* **343**, 393 (2014).
 - ²⁴ T. Wu *et al.*, *Nature Communications* **4**, 2113 (2013).
 - ²⁵ H. Li, R. T. Clay, and S. Mazumdar, *J. Phys.: Condens. Matter* **22**, 272201 (2010).
 - ²⁶ S. Dayal, R. T. Clay, H. Li, and S. Mazumdar, *Phys. Rev. B* **83**, 245106 (2011).
 - ²⁷ K. Mouloupoulos and N. W. Ashcroft, *Phys. Rev. Lett.* **69**, 2555 (1992).
 - ²⁸ N. Drichko, R. Beyer, E. Rose, M. Dressel, J. A. Schlueter, S. A. Turunova, E. I. Zhilyaeva, and R. N. Lyubovskaya, *Phys. Rev. B* **89**, 075133 (2014).
 - ²⁹ H. Gomi, T. Imai, A. Takahashi, and M. Aihara, *Phys. Rev. B* **82**, 035101 (2010).
 - ³⁰ M. Naka and S. Ishihara, *J. Phys. Soc. Jpn.* **79**, 063707 (2010).
 - ³¹ C. Hotta, *Phys. Rev. B* **82**, 241104 (2010).
 - ³² M. Abdel-Jawad, I. Terasaki, T. Sasaki, N. Yoneyama, N. Kobayashi, Y. Uesu, and C. Hotta, *Phys. Rev. B* **82**, 125119 (2010).
 - ³³ P. Lunkenheimer, J. Müller, S. Krohns, F. Schrettle, A. Loidl, B. Hartmann, R. Rommel, M. de Souza, C. Hotta, J. Schlueter, and M. Lang, *Nat. Mater.* **11**, 755 (2012).
 - ³⁴ K. Sedlmeier, S. Elsässer, D. Neubauer, R. Beyer, D. Wu, T. Ivek, S. Tomic, J. A. Schlueter, and M. Dressel, *Phys. Rev. B* **86**, 245103 (2012).
 - ³⁵ M. Dressel, P. Lazic, A. Pustogow, E. Zhukova, B. Gorshunov, J. A. Schlueter, O. Milat, B. Gumhalter, and S. Tomic, *Phys. Rev. B* **93**, 081201(R) (2016).
 - ³⁶ N. Gomes, W. W. De Silva, T. Dutta, R. T. Clay, and S. Mazumdar, *Phys. Rev. B* **93**, 165110 (2016).
 - ³⁷ H. Kino and H. Fukuyama, *J. Phys. Soc. Jpn.* **64**, 2726 (1995).
 - ³⁸ T. Mori, H. Mori, and S. Tanaka, *Bull. Chem. Soc. Jpn.* **72**, 179 (1999).
 - ³⁹ H. Oike, K. Miyagawa, H. Taniguchi, and K. Kanoda, *Phys. Rev. Lett.* **114**, 067002 (2015).
 - ⁴⁰ H. C. Kandpal, I. Opahle, Y.-Z. Zhang, H. O. Jeschke, and R. Valentí, *Phys. Rev. Lett.* **103**, 067004 (2009).

- ⁴¹ K. Nakamura, Y. Yoshimoto, T. Kosugi, R. Arita, and M. Imada, J. Phys. Soc. Jpn. **78**, 083710 (2009).
- ⁴² T. Koretsune and C. Hotta, Phys. Rev. B **89**, 045102 (2014).
- ⁴³ A. Painelli, A. Girlando, and A. Fortunelli, Phys. Rev. B **64**, 054509 (2001).
- ⁴⁴ See Supplemental Material at <http://link.aps.org/supplemental/xx.xxxx/PhysRevB.xxx.xxxxxx> for further details of calculations.
- ⁴⁵ T. Kashima and M. Imada, J. Phys. Soc. Jpn. **70**, 2287 (2001).
- ⁴⁶ S. Zhang, J. Carlson, and J. E. Gubernatis, Phys. Rev. B **55**, 7464 (1997).
- ⁴⁷ T. Mizusaki and M. Imada, Phys. Rev. B **69**, 125110 (2004).
- ⁴⁸ Z. B. Huang, H. Q. Lin, and J. E. Gubernatis, Phys. Rev. B **64**, 205101 (2001).
- ⁴⁹ H. Kino and H. Fukuyama, J. Phys. Soc. Jpn. **65**, 2158 (1996).
- ⁵⁰ K. R. Subbaswamy and M. Grabowski, Phys. Rev. B **24**, 2168 (1981).
- ⁵¹ S. Kivelson and D. Heim, Phys. Rev. B **26**, 4278 (1982).
- ⁵² S. Mazumdar and S. N. Dixit, Phys. Rev. Lett. **51**, 292 (1983).
- ⁵³ J. E. Hirsch, Phys. Rev. Lett. **51**, 296 (1983).
- ⁵⁴ S. Mazumdar and D. K. Campbell, Phys. Rev. Lett. **55**, 2067 (1985).
- ⁵⁵ R. Swietlik, A. Lapinski, M. Polomska, L. Ouahab, and J. Guillevis, Synth. Metals **133**, 273 (2003).
- ⁵⁶ A. Lapinski, R. Swietlik, L. Ouahab, and S. Golhen, J. Phys. Chem. A **117**, 5241 (2013).
- ⁵⁷ D. Andres, M. V. Kartsovnik, W. Biberacher, K. Neumaier, E. Schuberth, and H. Müller, Phys. Rev. B **72**, 174513 (2005).
- ⁵⁸ A. F. Bangura, A. I. Coldea, J. Singleton, A. Ardavan, A. Akutsu-Sato, H. Akutsu, S. S. Turner, P. Day, T. Yamamoto, and K. Yakushi, Phys. Rev. B **72**, 014543 (2005).
- ⁵⁹ M. Tamura, A. Nakao, and R. Kato, J. Phys. Soc. Jpn. **75**, 093701 (2006).
- ⁶⁰ T. Shikama *et al.*, Crystals **2**, 1502 (2012).
- ⁶¹ T. Holstein, Ann. Phys.(N.Y.) **8**, 325 (1959).
- ⁶² W. P. Su, J. R. Schrieffer, and A. J. Heeger, Phys. Rev. Lett. **42**, 1698 (1979).
- ⁶³ R. T. Clay, S. Mazumdar, and D. K. Campbell, Phys. Rev. B **67**, 115121 (2003).
- ⁶⁴ S. M. D. Soto, C. P. Slichter, A. M. Kini, H. H. Wang, U. Geiser, and J. M. Williams, Phys. Rev. B **52**, 10364 (1995).
- ⁶⁵ K. Miyagawa, K. Kanoda, and A. Kawamoto, Chem. Rev. **104**, 5635 (2004).
- ⁶⁶ O. J. Taylor, A. Carrington, and J. A. Schlueter, Phys. Rev. Lett. **99**, 057001 (2007).
- ⁶⁷ M. Pinterić, S. Tomić, M. Prester, D. Drobac, and K. Maki, Phys. Rev. B **66**, 174521 (2002).
- ⁶⁸ S. Milbradt, A. A. Bardin, C. J. S. Truncik, W. A. Huttema, A. C. Jacko, P. L. Burn, S.-C. Lo, B. J. Powell, and D. M. Broun, Phys. Rev. B **88**, 064501 (2013).
- ⁶⁹ N. V. Perunov, A. F. Shevchun, N. D. Kushch, and M. R. Trunin, JETP Letters **96**, 184 (2012).
- ⁷⁰ T. Arai, K. Ichimura, K. Nomura, S. Takasaki, J. Yamada, S. Nakatsuji, and H. Anzai, Phys. Rev. B **63**, 104518 (2001).
- ⁷¹ K. Ichimura, M. Takami, and K. Nomura, Journal of the Physical Society of Japan **77**, 114707 (2008).
- ⁷² Y. Oka, H. Nobukane, N. Matsunaga, K. Nomura, K. Katono, K. Ichimura, and A. Kawamoto, J. Phys. Soc. Jpn. **84**, 064713 (2015).
- ⁷³ J. M. Schrama, E. Rzepniewski, R. S. Edwards, J. Singleton, A. Ardavan, M. Kurmoo, and P. Day, Phys. Rev. Lett. **83**, 3041 (1999).
- ⁷⁴ L. Malone, O. J. Taylor, J. A. Schlueter, and A. Carrington, Phys. Rev. B **82**, 014522 (2010).
- ⁷⁵ K. Izawa, H. Yamaguchi, T. Sasaki, and Y. Matsuda, Phys. Rev. Lett. **88**, 027002 (2001).